Early-stage compositional segregation in polymer-blend films

H. Wang,[1,*] J. F. Douglas,[2] S. K. Satija,[2] R. J. Composto,[3] and C. C. Han[2]
[1]*Department of Materials Science and Engineering, Michigan Technological University, Michigan 49931, USA*
[2]*National Institute of Standards and Technology, Gaithersburg, Maryland 20899, USA*
[3]*Department of Materials Science and Engineering, Laboratory for Research on Structure of Matter, University of Pennsylvania, Philadelphia, Pennsylvania 19104, USA*
(Received 5 February 2003; published 23 June 2003)

The existence of a transient period during the surface enrichment of a binary polymer blend by one of its components has been suggested by previous theoretical and experimental studies as well as computer simulations. Taking advantage of the high depth resolution of neutron reflectivity and the slow dynamics of polymers near their glass transition, we investigate this early-stage surface compositional enrichment in a phase separating polymer blend for the first time. Two stages of surface enrichment layer growth are observed. A rapid local surface enrichment at the chain segmental level occurs first, followed by a slower growth of a diffuse layer having a scale on the order of the bulk correlation length and the radius of gyration of the surface enriching polymer chains.

DOI: 10.1103/PhysRevE.67.061801 PACS number(s): 36.20.−r, 68.08.Bc, 68.35.Fx

I. INTRODUCTION

The structure and properties of thin blend films is governed by an interplay between phase separation and surface segregation driven by polymer-surface interactions. This phenomenon is important for applications because commercial films normally comprise multiple polymer species, solvent, and additives, leading to numerous complex phase separation morphologies and to film properties that are difficult to control. The nature of the segregation depends on whether the mixture forms a stable one-phase fluid or phase separates [1–4]. In the one-phase regime, the surface enrichment layer (SEL) grows and stabilizes to an equilibrium value (''critical adsorption'') [5,6]. In the two-phase regime, the initially formed SEL for a bulk fluid in the presence of a boundary is unstable: it breaks into droplets for partial wetting and grows indefinitely for complete wetting [1]. However, under conditions of film confinement, the SEL can be stabilized against droplet formation for partial wetting, leading to a surface enrichment state near the boundary much like critical adsorption [7,8]. For complete wetting, the SEL coarsens at rates varying from logarithmic to power-law growth (exponents between 0.1 and 1) [7–20]. Thus, the late-stage evolution of the SEL exhibits ''nonuniversal'' growth laws, dependent on the phase stability, wetting characteristics of the film, confinement, as well as the details of the polymer-surface interaction potential [2,14]. We can expect that hydrodynamic effects, which generally complicate late-stage phase separation, wetting and dewetting processes, will have little effect on the early-stage of surface segregation where the SEL first forms, and thus there is a better chance for observing ''universal'' kinetic growth in this growth regime for surfaces with van der Waals interactions between the fluid and the environment. Notably, the growth of compositional enrichment of the surface layer occurs in both the one- and two-phase regions, so we can expect the process of forming a SEL layer in a wetting or prewetting phase, separating fluid mixture to be similar, if not identical, to the growth of critical absorption layers in miscible fluids.

While many previous measurements have focused on the late-stage evolution of the SEL [13–20], there has been no investigation of the early-stage of growth during which these layers first form. The existence of this transient early stage, however, has been suggested by numerous previous studies. A general feature of past measurements [13–20] and simulations [7–11] is that the extrapolation of the SEL thickness to the initial time ($t=0$) gives a nonzero intercept, suggesting rapid changes in the surface composition profiles at early times [7,8]. This transient behavior eluded experimental investigation because for polymer melts the time scale involved is typically short (well below 1 min) and the length scale is small. On the other hand, continuum models of phase separation cannot describe this regime because physical processes smaller than the coarse graining scale (correlation length for phase separation) are involved, while the time scales required for phase separation in polymer systems are long for molecular dynamics simulation.

We therefore designed a measurement that can access the short time and small length-scale surface enrichment regime. In this study, a critical blend film near the glass transition of the polymers is utilized so that the chain dynamics is greatly slowed down even under thermodynamically strong segregation conditions. These measurements reveal two metastable stages of surface segregation in the growth of the SEL, corresponding to a rapid local surface enrichment at the chain segmental level followed by a slower growth of a diffuse layer having a scale on the order of the bulk correlation length and the radius of gyration of surface enriching polymer chains.

II. MATERIALS AND EXPERIMENTS

The polymers are deuterated poly(methyl methacrylate) (dPMMA, $M_w=51$ kg/mol, PD$=1.04$) and poly(styrene-ran-acrylonitrile) (SAN, 33% AN by mass, M_w

*Corresponding author. Email address: wangh@mtu.edu

=124 124 kg/mol. PD=2.24) [21]. The SAN polymer was received from Monsanto Chemical Company [21] and was purified three times through solution precipitation for removing oligomers and other impurities. The dPMMA, which was synthesized and purifed by the vendor Polymer Source Inc [21], was used as received. At a scan rate of 10 °C/min, differential scanning calorimetry shows a glass transition T_g around 120 °C for dPMMA and 114 °C for SAN, respectively. Blends of PMMA and SAN can exhibit a lower critical solution temperature (LCST) in certain comonomer composition ranges in SAN [22,23].

Small angle neutron scattering (SANS) was used to probe the LCST of the blend. Blends of various compositions were prepared by slowly evaporating the solvent from solutions in methyl isoamyl ketone (MIAK) at room temperature, followed by drying in a vacuum oven at 120 °C for 48 h. The blends were then pressed to form disks of 1 mm thickness at 125 °C. The blend with a dPMMA volume fraction, $\phi_{dPMMA}=0.19$, was clear and transparent, showing one-phase characteristics, whereas the others at $\phi_{dPMMA}=0.29,0.38,0.48$, and 0.57 were all opaque, implying that phase separation had already occured. SANS measurements were performed using the 8-m SANS instrument at the NIST Center for Neutron Research (NCNR). Incident neutrons had wavelength of $\lambda=10$ Å with a dispersion, $\Delta\lambda/\lambda=0.15$. The samples were equilibrated at measurement temperatures for 60 min before the SANS measurements were made. The scattered neutrons were counted with a 2D detector, and the scattering intensity was radially averaged and reduced to the absolute scale using a 1-mm thick silica sample as an intensity standard.

A film of dPMMA-SAN (50-50 by mass) was obtained by spin casting from a 2% (by mass) common solution in MIAK on a clean silicon oxide substrate. The substrate was prepared as follows: after cleaning the substrate by both boiling acid and base wash, the native oxide layer was then etched using buffered HF solution and an oxide layer of 15 Å was reintroduced by oxygen plasma treatment for 5 min. The film was then dried in vacuum oven at 120 ± 2 °C, which is around the glass transition temperature of dPMMA, for 2 h, then kept at 100 ± 2 °C overnight. X-ray reflectivity (XR) was used to monitor the thickness variation of a reference sample after successive annealing at 120 °C, ensuring the complete removal of the residual solvent in samples used for the current study. After drying, the sample film thickness was measured by XR and fit as a single layer to equal 445 ± 2 Å, which remains constant thoughout the subsequent annealing. The dPMMA volume fraction was estimated to equal $\phi_{0,dPMMA}=0.48$.

The films were annealed at 130 ± 0.1 °C in a vacuum oven, which was designed and constructed in the Polymers Division at the National Institute of Standards and Technology, and allowed for precise temperature control to be within a fraction of a degree over a large volume. A large brass block was preequilibrated in the oven, the sample was then quickly transfered to a sample slot in the metal block to be encapsulated. After annealing, the sample was transfered quickly to another brass block at room temperature as a heat sink. To enhance the contact between the metal blocks and the silicon wafer, the contacting brass surfaces were well polished to be both flat and smooth. To obtain the precise annealing time, a thermal couple was soldered to the surface of a silicon wafer with the same thermal mass, and the raise and drop of the surface temperature of the wafer following the same annealing treatment was monitored. The corrected annealing times in this study range from 65 s to 36 h, with an uncertainty of ± 5 s. The film after each step of annealing was measured, using neutron reflectivity (NR) at the NG7 reflectometer at the NCNR. The reflectance R as a function of the half of the momentum transfer, $k=2\pi\sin\theta/\lambda$ (with 2θ the scattering angle and $\lambda=4.75$ Å), was recorded with a point detector. Atomic force microscopy (AFM) measurements indicated that the root-mean-square roughness of the film was below 6 Å during all stages of preparation, drying, annealing, and measurements. Fitting the NR data further confirmed that this roughness value is a macroscopic quantity.

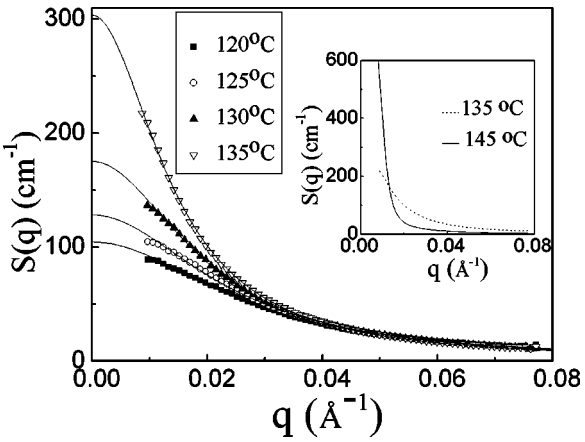

FIG. 1. SANS scattering intensity for a dPMMA-SAN blend with $\phi_{dPMMA}=0.19$ at various temperatures below the spinodal temperature. The solid curves are the best fits using random-phase approximation. The inset shows that the scattering intensity at low-q diverges upon spinodal decomposition at 145 °C while remains finite in one-phase regime at 135 °C.

III. RESULTS AND DISCUSSIONS

Figure 1 shows the SANS measurement of static structure factors $S(q)$ for a blend with $\phi_{dPMMA}=0.19$ at various temperatures. $S(q)$ increases with temperature implying phase separation upon heating. In the low-q limit, de Gennes's random-phase approximation (RPA) can be expanded to give the classical Ornstern-Zernike equation for concentration fluctuations

$$S(q)=\frac{S(0)}{1+\xi_b^2 q^2}, \tag{1}$$

where ξ_b is the bulk correlation length of the density fluctuation. The solid curves in Fig. 1 are the best fits using Eq. (1), giving both the $S(0)$ and the ξ_b at various temperatures. Figure 2 shows that both $S(0)^{-1}$ and ξ_b^{-2} scales linearly

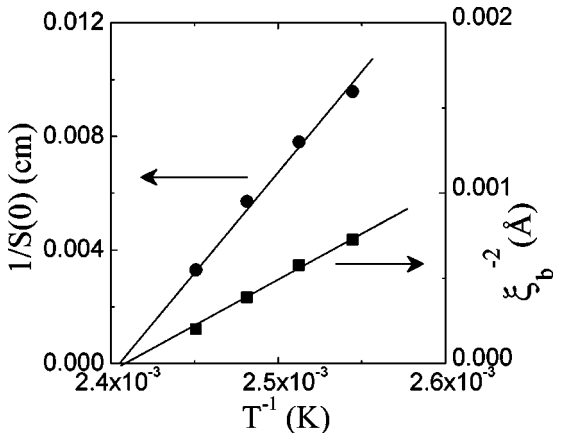

FIG. 2. The inverse of the zero-angle structure factor and the inverse of the square of the bulk correlation length as a function of the inverse temperature. Linear fits with extrapolations give $T_s = 141\,^{\circ}\mathrm{C}$. The standard errors of the data in this plot are smaller than the symbol size.

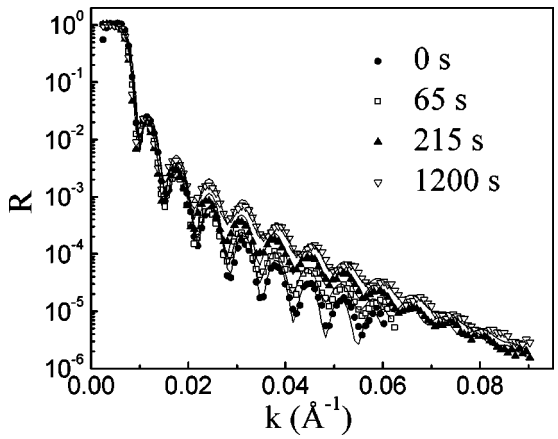

FIG. 3. Selected neutron reflectivity spectra after 0 s (circles), 65 s (squares), 215 s (uptriangles) and 1200 s (downtriangles) at 130 °C show increasing reflectance at high k with annealing. The solid curves are the best fit to the data based on the model described in the text.

with the inverse absolute temperature, as predicted by the mean-field theory. At the spinodal temperature, both concentration fluctuations and the correlation length diverge. Linear fitting of the data then extrapolating to $S(0)^{-1}=0$ and $\xi_b^{-2}=0$ gives spinodal temperature $T_s=141\,^{\circ}\mathrm{C}$ for the blend with $\phi_{dPMMA}=0.19$. All other blends prepared for the SANS study, with $\phi_{dPMMA}=0.29$ and higher, show phase-separated characteristics at 125 °C and higher temperatures. A comparison between the structure factors in two-phase and in one-phase regimes is shown in the inset of Fig. 1.

The bulk correlation length for density fluctuations in one-phase regime is related to the interaction parameter through

$$\xi_b^2=\frac{b^2}{36}[\phi_1\phi_2(\chi_s-\chi)]^{-1}, \tag{2}$$

where b is the average statistic segment length, χ is the interaction parameter, χ_s is the critical value for spinodal decomposition, and ϕ_1 and ϕ_2 are the volume fractions of the two polymers, respectively. From the $\xi_b(T)$ data, the interaction parameter can be estimated, $\chi=(0.118-43.1)/T$, assuming an average segment length of 6.5 Å. In two-phase regime, the correlation length characterizing the dominant wavelength during the early stage of spinodal decomposition is given by [24]

$$\xi_k^2=\tfrac{2}{3}R_g^2[\chi_s/(\chi-\chi_s)], \tag{3}$$

where R_g is the radius of gyration of unperturbed polymer chains. Assuming that the volume fraction dependence of χ is small, we used the above χ value to estimate both the spinodal temperature and the correlation length of the blend for the surface segregation study. At $\phi_{dPMMA}=0.48$, the spinodal temperature of the blend is estimated to be *ca.* 115 °C, and the correlation length $\xi_k(130\,^{\circ}\mathrm{C})=39$ Å. By choosing a blend with a phase separation temperature between the room temperature and the glass transition temperature, it is possible to prepare homogeneous films through spin casting and slow down the kinetics of the phase separation by annealing just above T_g. Figure 3 shows NR spectra of the $\phi_{dPMMA}=0.48$ blend after annealing at 130 °C for 0 s, 65 s, 215 s, and 1200 s. The reflectance at higher k increases with time, indicating segregation of dPMMA to the surface. The spectra were analyzed using a model-fitting scheme: the wetting layers at both the surface and the silicon substrate are described using stretched exponential profiles [25–27], and are followed by depletion zones that we describe by error function-type composition profiles. The bulk composition is held at the as-cast value 0.48. We fit the near-surface profile using

$$\phi(x)=\phi_d+(\phi_s-\phi_d)e^{-(x/\xi_s)^2}, \tag{4}$$

where $\phi(x)$ is the composition and x is the depth from the surface; ϕ_s and ϕ_d are the dPMMA compositions at the surface and of the depletion layer, respectively; ξ_s denotes the surface correlation length. An equivalent set of parameters is also used to describe the profiles near the silicon substrate. Mass conservation at both the surface and substrate has been ensured during the fitting. An alternative model using a damped oscillatory profile (as typically observed for surface-directed spinodal decomposition [28]) has also been compared to the data. However, the fit does not converge to the oscillatory profile. The validity of model-fitting scheme was further confirmed by both a model-free fitting method (parametric *B*-spine approach) [29] and a set of independent neutron reflection measurements on one sample for direct inversion (i.e., obtaining phase factors from the experimental data hence calculating the depth profile directly) [30]. The best fits of the NR spectra are shown as the solid lines through symbols, and their corresponding compositional profiles are shown in Fig. 4. As the film thickness remains constant throughout the entire measurement, the shift of fringes reflects the interference with the internal interfaces developed during the surface segregation. It is evident that at both the surface and the interface, the amount of wetting component

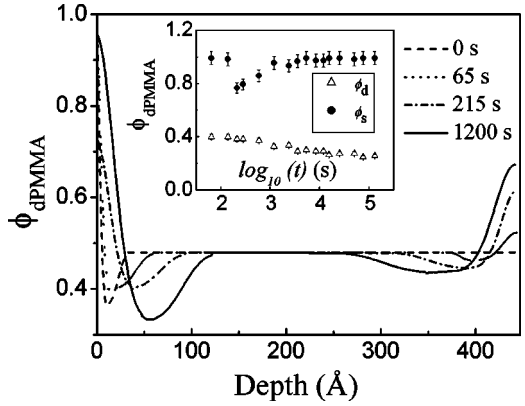

FIG. 4. dPMMA compositional depth profiles give the best fit of NR spectra shown in Fig. 3. The inset shows the evolution of surface composition ϕ_s (circles) and depletion layer composition ϕ_d (triangles).

increases, and the depletion zone broadens with time. The inset of Fig. 4 shows the evolution of ϕ_d and ϕ_s. The former decreases monotonically, suggesting that equilibrium has not been achieved, while the latter decreases first and then increases to saturate at a value close to unity. This nonmonotonic variation for ϕ_s coincides with the rapid initial increase in ξ_s, as discussed later.

The surface excess, defined as a scale of surface enrichment, is given as

$$z^* = \int [\phi(x) - \phi_d] dx. \tag{5}$$

Figure 5 shows z^* as a function of annealing time in log-log scales over more than three decades. This plot, however, does not include the measurement for $t=0$ (i.e., right after the drying), which shows $z^*=4$ Å, a value corresponding to a segmental scale coverage. This initial state comes from nonequilibrium processing conditions such as spin-casting

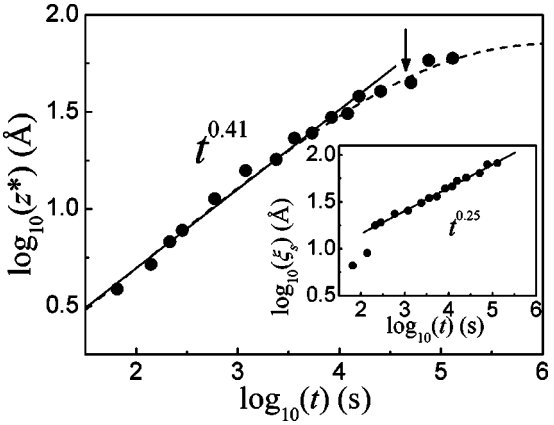

FIG. 5. Surface excess z^* as a function of annealing time in double $\log_{10}$ scales. The line indicates power-law fit, $t^{0.41\pm0.01}$, and the dashed curve is a fit to the stretched exponential function described by Eq. (6). The inset shows the surface correlation length ξ_s as a function of time. The line represents a power-law growth of $t^{0.25\pm0.01}$.

and solvent evaporation; however, no larger-scale segregation, such as phase separation, occurs during the sample preparation, as evident by the smoothness of the film. The metastable surface segregation of dPMMA monomer at a segmental scale is probably ubiquitous in all polymer blends with preferential surface interaction. At later times, the evolution of z^* can be fit to a power law $t^{0.41\pm0.01}$ for early times (solid line), but there seems to be definite tendency for z^* to level off at long times. Accordingly, we have also fit our data to a stretched exponential form

$$z^*(t) = z^*(\infty)[1 - e^{-(t/\tau)^{0.41}}], \tag{6}$$

which has the saturation effect built into it, as shown by the dashed curve in Fig. 5. This form was previously introduced to describe diffusion-limited polymer adsorption with saturation of coverage at long times [31–33]. The best fit gives $z^*(\infty)=72$ Å. The power-law growth kinetics is due to diffusive segregation of polymer chains under the influence of the surface interaction. The kinetic slowing down does not imply that the material enriching the surface is depleted from the bulk of the film. The best-fit composition profile obtained from the NR after 16 h (arrow in Fig. 5) shows that the bulk of the film remains near the as-cast composition. This observation indicates that reasons other than depletion of the wetting material are responsible for the slowing down in the growth rate at long times. Note that z^* starts to deviate from the power-law behavior at about 9 h corresponding to $z^*=40$ Å and $\xi_s=57$ Å. These scales are comparable to the bulk correlation length, $\xi_k=39$ Å, suggesting a transient saturation in the growth of SEL layer, in accord with theoretical modeling [7–12]. The complete formation of the surface enrichment layer sets the stage for later stages of evolution just as the early stage of bulk phase separation sets up the later state morphological development. Once formed, the SEL may remain stationary, break into droplets, or grow indefinitely at a rate that depends on the quench depth and the relative polymer-surface interaction (i.e., surface field [1,7,8,14,34]). In the case of strong wetting, as for dPMMA at the surface in this study, the SEL will grow to a thick wetting layer after transient saturation, as documented previously [13]. However, this late stage of surface segregation is too slow at 130 °C to be accessible in the current study.

The thickness of the SEL at long times in this study could have another interpretation. The R_g of dPMMA in the melt ($\approx$37 Å) is also comparable to the length scale of the SEL thickness at the kinetics crossover ($z^*=40$ Å). Given this coincidence, it is not clear whether the scale of the SEL at long times in Fig. 5 reflects the transient formation of a polymer layer of dPMMA having molecular dimensions or a transient layer having a thickness comparable to ξ_k. This question can only be resolved by comparing the saturation scale of ξ_s (or z^*) to ξ_k over a temperature range near the critical point for phase separation. Although measurements of this kind are rare [6,26], they suggest that ξ_s (or z^*) should be comparable to ξ_k far away from criticality, but $\xi_k \gg \xi_s$ near the critical point. This is consistent with our measurements, which were conducted well within the two-phase regime.

Another imporant quantity describing the SEL is ξ_s. The inset of Fig. 5 shows that ξ_s nearly follows a power law of $t^{0.25\pm0.01}$, except for initial times. Probably due to the small exponent for the power-law growth, a leveling off at later times is not practically accessible, but this saturation is certainly expected to exist as for z^*. While most theoretical studies and simulations focus on the kinetics after the formation of an initial layer with thickness ξ_k [7–12], this transient early-stage of SEL has received little attention so that the interpretation of this apparent power-law growth will require further investigation. A rather intriguing observation is the rapid increase of ξ_s at early times, which coincides with the sharp variation in ϕ_s at about 100 s. We suggest that since a highly nonequilibrium segmental adsorption layer of dPMMA is formed during the process of solution spin casting and subsequent drying, the film responds initially to the annealing in the melt by adjusting its surface concentration to obtain a local equilibrium at the segmental level. This process may be responsible for the sharp variation in both ξ_s and ϕ_s.

There have been no previous quantitative investigations of molecular scale composition change occurring near the surface of spun-cast films, since these compositional changes are normally too rapid to observe. Taking advantage of the high depth resolution of neutron reflectivity and slow dynamics of polymers near their glass transitions, we are able to investigate the very early stage of surface compositional enrichment in a phase separating dPMMA-SAN blend. We find two distinct surface saturation states corresponding to the polymer's two characteristic length scales, the segmental size and the chain radius of gyration. Segregation at a monomer length scale requires only small-scale displacements and thus this process is very fast. The growth of a SEL with a scale comparable to R_g requires the chain center of mass to diffuse a distance $O(R_g)$. In a situation when R_g differs from ξ_k, a three-step process is possible for polymers. In a small molecule fluid mixture near its criticality, however, only two-step process can be expected: a single layer deposition at the solid substrate followed by the growth of a SEL on the order of ξ_k. It is not clear how chain connectivity alters the nature of SEL formation in polymers. Further studies on SEL growth in both small molecule and polymer fluids will be required to answer this important question.

The two-stage process of SEL growth shown in this study, however, occured within the initial transient period of many previous studies [13–20] and should not be mistaken with the two stages involving a crossover from the transient period to the late stage behavior. A useful criterion is whether the crossover occurs at a length scale $O(R_g)$. This criterion, however, can find its applications beyond the surface segregation and wetting phenomena. For example, previous experiments on polymer-polymer interdiffusion also showed that the development of the interfacial width follows different growth exponents at the early and later times [35,36]. The transition occurs at the reptation time, which is defined as the time necessary for polymer chains to diffuse a distance $O(R_g)$. The diffusion at the polymer-polymer interface is quite different from that close to the surface. In the former, the entropic restoring force that drives the rapid initial interfacial relaxation is important, whereas in the latter, surface interaction dominates the initial kinetics.

IV. SUMMARY

In this study, we take advantage of the high depth resolution of neutron reflectivity and the slow dynamics of polymers near their glass transition, and investigate the early-stage surface compositional enrichment in a phase separating polymer blend for the first time. Two stages of surface enrichment layer growth are observed. A rapid local surface enrichment at the chain segmental level occurs first, followed by a slower growth of a diffuse layer having a scale on the order of the bulk correlation length and the radius of gyration of the surface preferred component. Those two processes are within the elusive transient period suggested by previous studies. The present study is to quantitatively examine this important phenomenon in a polymer blend in two-phase regime. As still little is known about this phenomenon, in this paper, we present an initial exploratory experiment and hope to stimulate further studies on this subject.

ACKNOWLEDGMENTS

H.W. acknowledges the start-up fund from the Michigan Technological University, and R.J.C. acknowledges financial support from the NSF DMR Polymer Program, Grant No. DMR-0234903.

[1] S. Dietrich, *Phase Transition and Critical Phenomena* (Academic Press, London, 1988), Vol. 12.
[2] K. Binder, J. Non-Equil. Thermodyn. **23**, 1 (1998), and references therein.
[3] G. Krausch, Mater. Sci. Eng., R. **14**, 1 (1995).
[4] M. Geoghegan and G. Krausch, Prog. Polym. Sci. **28**, 261 (2003).
[5] R.A.L. Jones, E.J. Kramer, M.H. Rafailovich, J. Sokolov, and S.A. Schwarz, Phys. Rev. Lett. **62**, 280 (1989).
[6] J. Genzer and R.J. Composto, Europhys. Lett. **38**, 171 (1997).
[7] S. Puri and K. Binder, J. Stat. Phys. **77**, 145 (1994).
[8] S. Puri and K. Binder, Phys. Rev. E **49**, 5359 (1994).
[9] G. Brown and A. Chakrabarti, Phys. Rev. A **46**, 4829 (1992).
[10] H. Chen and A. Chakrabarti, Phys. Rev. E **55**, 5680 (1997).
[11] S. Bastea, S. Puri, and J.L. Lebowitz, Phys. Rev. E **63**, 041513 (2001).
[12] R. Lipowsky and D.A. Huse, Phys. Rev. Lett. **57**, 353 (1986).
[13] H. Wang and R.J. Composto, Phys. Rev. E **61**, 1659 (2000).
[14] M. Geoghegan, H. Ermer, G. Jungst, G. Krausch, and R. Brenn, Phys. Rev. E **62**, 940 (2000).
[15] H. Tanaka, Phys. Rev. Lett. **70**, 53 (1993).
[16] H. Tanaka, Phys. Rev. Lett. **70**, 2770 (1993).
[17] G. Krausch, C.A. Dai, E.J. Kramer, and F.S. Bates, Phys. Rev. Lett. **71**, 3669 (1993).

[18] U. Steiner, J. Klein, E.J. Eiser, A. Budkowski, and L. Fetters, Science **258**, 1126 (1992).
[19] U. Steiner and J. Klein, Phys. Rev. Lett. **77**, 2526 (1996).
[20] P. Guenoun, D. Beysens, and M. Robert, Phys. Rev. Lett. **65**, 2406 (1990).
[21] The references to commercial equipment or materials do not imply recommendation or endorsement by the National Institute of Standards and Technology.
[22] M.E. Fowler, J.W. Barlow, and D.R. Paul, Polymer **28**, 1177 (1987).
[23] M. Suess, J. Kressler, and M. Kammer, Polymer **28**, 957 (1987).
[24] P.G. deGennes, J. Chem. Phys. **72**, 4756 (1980).
[25] R.A.L. Jones *et al.*, Europhys. Lett. **12**, 41 (1990).
[26] H. Grüll *et al.* (unpublished).
[27] K.F. Freed, J. Chem. Phys. **105**, 10 572 (1996).
[28] R.A.L. Jones, L.J. Norton, E.J. Kramer, F.S. Bates, and P. Wiltzius, Phys. Rev. Lett. **66**, 1326 (1991).
[29] N.F. Berk and C.F. Majkrzak, Phys. Rev. B **51**, 11 296 (1995).
[30] C.F. Majkrzak, N.F. Berk, J. Dura, S.K. Satija, A. Karim, J. Pedulla, and R.D. Deslattes, Physica B **248**, 338 (1998).
[31] J.F. Douglas, H.E. Johnson, and S. Granick, Science **262**, 2010 (1993).
[32] J.P. Wilcoxon, J.E. Martin, and J. Odinek, Phys. Rev. Lett. **75**, 1558 (1995).
[33] A.N. Emerton, P.V. Coveney, and B.M. Boghosian, Phys. Rev. E **55**, 708 (1997).
[34] K.B.S. Puri, Phys. Rev. Lett. **86**, 1797 (2001).
[35] G.P. Felcher, A. Karim, and T.P. Russell, J. Non-Cryst. Solids **131**, 703 (1991).
[36] G. Reiter and U. Steiner, J. Phys. II **1**, 659 (1991).